Journal of Applied Polymer Science

Aerogel of Nitrate Glycerol Ether Cellulose Based on Phase Separation in Acetone/Ethanol Mixed Solvents System

Yunhua Zhang,[1] Ziqiang Shao,[1,2] Jia Li,[1] Kezheng Gao,[1] Yanhua Liu[2]
[1]School of Materials Science and Engineering, Beijing Institute of Technology, Beijing 100081, China
[2]North Century Cellulose Technology Research & Development. Co. LTD, Beijing, China
Correspondence to: Z. Shao (E-mail: shaoziqiang@263.net)

ABSTRACT: Nitrate glycerol ether cellulose (NGEC) alcogels are formed in the ternary NGEC/acetone/ethanol system. NGEC aerogels are prepared from NGEC alcogels after solvent exchange and drying under supercritical CO_2 ($scCO_2$). The aerogels are prepared with various densities and porosities, relating directly to the initial ethanol content. NGEC aerogels had surface areas of up to 183 m^2 g^{-1} and large mesopore volumes with a combination of large macropore volumes and a wide range of mesopore sizes. The aerogels with larger pore size distribution range, average pore diameter, and mesopore and macropore volume were obtained from system with higher ethanol content. The aerogels were further characterized by X-ray diffraction, Brunauer–Emmett–Teller analysis, electron microscopy, and thermogravimetric analysis. The results showed that the NGEC aerogels clearly retained the crystalline structure from NGEC. Compared with NGEC powders, the thermal decomposition of NGEC aerogel is accelerated and this process becomes more acute. © 2014 Wiley Periodicals, Inc. J. Appl. Polym. Sci. **2015**, *132*, 41405.

KEYWORDS: Nitrate glycerol ether cellulose; NGEC alcogel; NGEC aerogel; phase separation

Received 31 March 2014; accepted 18 August 2014
DOI: 10.1002/app.41405

INTRODUCTION

Extensive interest has already focused on aerogels, a well developed and diverse class of porous materials, because their pore structure and high special surface area play an important role in enabling high activity for any heterogeneous application, such as sensing, catalysis, and adsorption of gases.[1–5] As Kistler reported the first aerogels, different types of organic and inorganic aerogels have been made and are successfully used in various applications such as catalytic, electrochemical, separations, and sensing.[6–9] Within the range of organic aerogels, aerogels with high surface area made from natural materials have been reported.[10–12] Recently, studies on cellulose or cellulose derivatives aerogels, has sharply increased because cellulose is one of the most abundant and renewable natural polymers. We are now devoted to the formulation of a new class of aerogels prepared with a novel cellulose nitrate derivative.

Recently, nitrate glycerol ether cellulose (NGEC), a novel cellulose nitrate with small molecule branch chains in the big molecule main chain of NGEC which can improve its molecular flexibility, has been synthesized in our lab.[13–15] Because of the similar physical and chemical properties compared to NC, NGEC can be used instead of NC in many applications for typical NC, such as applications in gas generators, propellants, coatings, printing inks, filtration, and membranes for immunoassays, enzyme immobilization, biosensors, and the isolation of proteins, RNA, and DNA.[16–19]

To date, many studies found that the morphology (surface area) of a material obviously effect its properties and applications.[20–23] Therefore, by preparing NGEC gels materials may significantly increase the surface area and broaden applications in explosives and propellants, separations, purification science, and biomedicine. Recently, the preparation and the viscoelastic behavior of NGEC alcogels formed in a mixed NGEC/acetone/ethanol solvent system were reported.[24] Herein, we further report, for the first time, NGEC aerogels are obtained from NGEC alcogel after solvent exchange with ethanol and drying under supercritical CO_2. We focus on the influence of the initial solvent composition on morphology of NGEC aerogel.

EXPERIMENTAL

Materials

Cellulose M60 obtained from North Century Cellulose Technology Research & Development (Beijing, China). NGEC (nitrogen content = 12.88 wt %, DS = 2.87) was prepared by nitration of cellulose glycerol ether (MS = 0.3) in our lab. The nitration reaction was expected to proceed as shown in Scheme 1. Nitric acid was of 97% purity, dichloromethane was of 98% analytical grade, ethanol was of 99.98% purity, acetone was of 99.98%

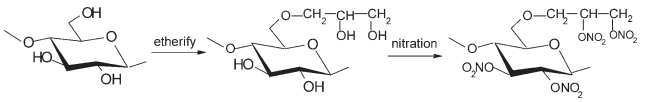

Scheme 1. The mechanism of nitration.

purity, isopropanol was of 98% analytical grade, and glycidol was of 99.98% purity (Beijing Chemical Agent) were used as received.

Preparation of NGEC aerogel

The NGEC powder was added into different ratio of acetone/ethanol (w/w = 3/1, 2/1, 1/1, and 2/3) with the certain NGEC concentration 2.5 wt %. The mixture stirred at room temperature for several hours to get clear solutions. NGEC alcogels were prepared by partial solvent evaporation of the NGEC solution.[24] For convenience, the NGEC gels formed in acetone/ethanol (w/w = 3/1, 2/1, 1/1 and 2/3) with certain NGEC concentration 2.5 wt % were coded as NGC1, NGC2, NGC3, NGC4. The gel was further turned into excess anhydrous ethanol under stirring, changing the ethanol with fresh one every day for 4 days at room temperature, to replace the solvent within the network of the gel to obtain NGEC alcogel. The alcogels were dried with supercritical CO_2 to obtain the NGEC aerogels (Figure 1). Drying in CO_2 supercritical conditions was performed using an automatic critical point dryer apparatus (Applied Separations). Samples were placed in 5 L autoclave filled with absolute ethanol to avoid evaporation before the beginning of the process. The system was closed and cooled to 5°C, pressurized to 5.5 MPa with pure liquid CO_2. The excess of ethanol was purged by liquid CO_2, maintaining the pressure and the temperature constant for 1 h. Filling and purging steps were repeated four times to be sure that ethanol was completely replaced by liquid CO_2. After these cycles, the system was pressurized until the operating conditions were reached: 16 MPa and 50°C, and was maintained for 30 min. Then, the system was slowly depressurized at a controlled rate (0.5 MPa/h) to avoid condensation of liquid CO_2 and the phenomenon of cracking. Once the atmospheric pressure was reached, the system was cooled down to the ambient temperature and the autoclave was opened. After these steps, NGEC aerogels were obtained.

Scanning Electron Microscopy

The morphologies of the aerogels were examined via a S4800 scanning electron microscope (SEM; Hitachi, Japan) at an accelerating voltage of 2 kV. The samples were sputter-coated with a thin layer of gold (15 mA coating current for 1 min) before imaging to ensure good conductivity and imaging.

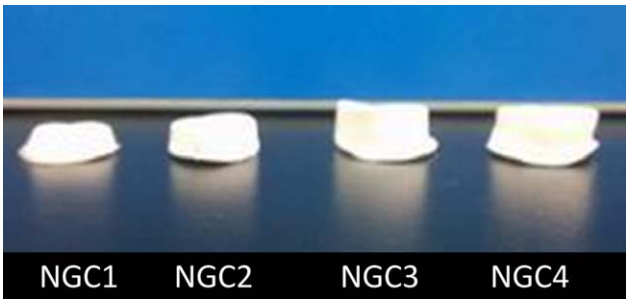

Figure 1. Macroscopic view of NGEC aerogels formed in the initial solutions with different acetone/ethanol ratios (sample codes of NGEC are shown below each vial). [Color figure can be viewed in the online issue, which is available at wileyonlinelibrary.com.]

Densities and Porosities of NGEC Gels

Densities of the samples were calculated by measuring their dimensions using a digital caliper (0.02 mm) and weighing the aerogels on an analytical balance (0.01 mg accuracy). Five different positions for each aerogel sample were taken at to measure the dimensions. Percentage porosity of the sample (P) was determined using the density of the samples (d_a) and the density of the NGEC powders ($d_p = 1.68$ gcm^{-3}). The percentage porosity can be calculated by Eq. (1):

$$P = \left(1 - d_a/d_p\right) * 100\% \quad (1)$$

X-ray Diffraction

Powder X-ray diffraction (XRD) data was recorded on a D8 Advance (Bruker, Germany) X-ray diffractometer (40 kV, 40 mA) with Cu K_α radiation (wavelength = 0.154 nm) with a step interval of 0.02°, time per step 0.6 s.

Nitrogen Adsorption Measurement

The measurements of aerocellulose porosity (pores size and their distribution, specific surface) were performed with an ASAP 2010 (Micromeritics) to obtain texture properties. The pore size was investigated in the range from 0.05 to 100 nm by N_2 sorption. The BET analysis was calculated in the relative pressure range from 0.06 to 0.35, measurements were performed at 77 K. The Barrett–Joyner–Halenda (BJH) analysis was

Table I. Properties of NGEC Aerogels

Samples codes	ρ (g cm^{-3})	%porosity	S_{BET} (m^2 g^{-1})	V_{total} (cm^3 g^{-1})	V_{meso} (cm^3 g^{-1})	% mesopore	2r (nm)
NGC1	0.179	89.34	142 ± 4	0.51 ± 0.01	0.38 ± 0.01	73.93	13.8
NGC2	0.133	92.01	158 ± 7	0.75 ± 0.01	0.53 ± 0.01	70.55	16.8
NGC3	0.106	93.69	171 ± 5	0.91 ± 0.01	0.55 ± 0.01	60.29	22.6
NGC4	0.082	95.12	183 ± 6	0.98 ± 0.01	0.56 ± 0.01	56.94	23.0

The ρ is the density of aerogels; %porosity is the percentage porosity of aerogels; S_{BET} is the BET surface area calculated using the amount of N_2 adsorbed at a relative vapour pressure of 0.06–0.35 at 77 K. V_{total} is the total pore volume determined at P/P_0 of 0.99; V_{meso} is the mesopore volume determined at P/P_0 of 0.95; % mesopore volume is the percentage of the total pore volume that is mesoporous; 2r is the average pore diameter of the aerogels determined using the desorption branch of the isotherm, using the BJH method.

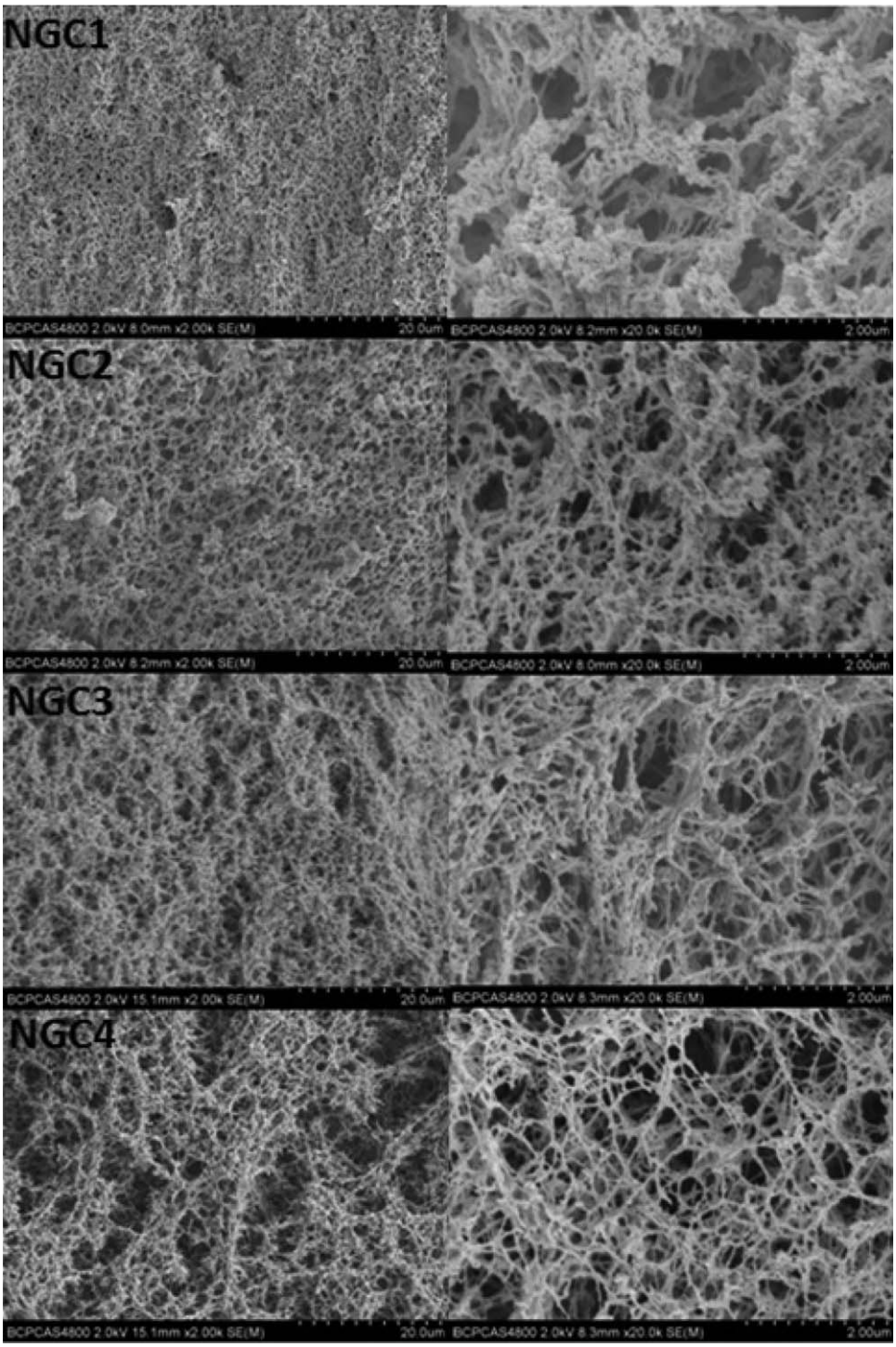

Figure 2. SEM images of NGEC aerogel prepared at various acetone/ethanol ratios (left: (2000k), right : 20,000k).

performed using the desorption branch of the isotherms. Measurement for each sample was repeated three times.

TG–DTG Measurement

TG–DTG curves under the condition of flowing nitrogen gas (purity, 99.999%; atmospheric pressure) were obtained using a TA2950 thermal analyzer (TA), and the conditions were: sample mass, about 1 mg; N_2 flowing rate, 40 cm^3 min^{-1}; heating rates, 10 and 1 K min^{-1}.

RESULTS AND DISCUSSION

Gelation of NGEC/acetone/ethanol solution with different initial acetone/ethanol ratios and NGEC concentrations was reported in detail in Ref. 24. Here, we present the main results of the influence of acetone/ethanol ratios on NGEC gels studied. The final acetone/ethanol ratios of all NGEC gels are around 30/70. The NGEC/acetone/ethanol ternary system with more ethanol content requires less time for less evaporated solvent to get the

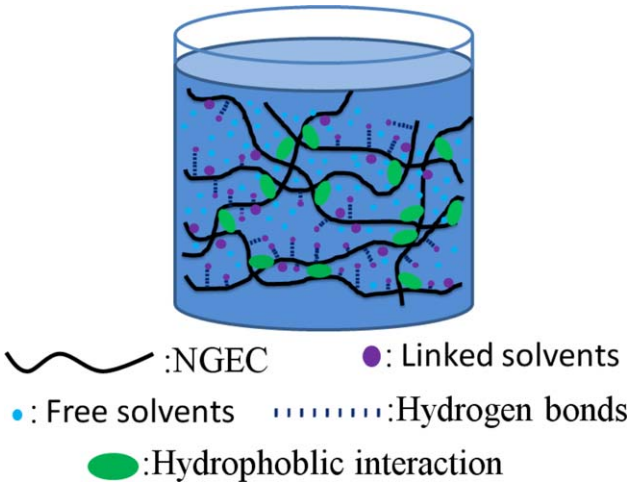

Figure 3. Mechanism of the sol–gel transition for the NGEC/acetone/ethanol ternary system. [Color figure can be viewed in the online issue, which is available at wileyonlinelibrary.com.]

gel point, and a lower dense NGEC gel with larger volume/weight is formed from this ternary system. After solvent exchange with ethanol and drying under supercritical CO_2 ($scCO_2$) described in Methods section, white dry pure NGEC samples, NGEC aerogels with different volumes, were obtained (Figure 1). The total shrinkage of the samples was lower than 20% as compared with the initial volume of the alcogel. The density of the aerogels decreased as the initial ethanol content in the NGEC solution increasing. As expected, there was an associated increase in porosity with a decrease in aerogel density [eq. (1)], from 89.34 to 95.12% (Table I).

Porous network structure of the aerogels was imaged via SEM. Figure 2 shows representative images taken of NGEC aerogels at two different magnifications. The lower magnification image (left column of Figure 2) shows that the trend in changing surface areas corresponds to a shift in gel morphology from a more homogeneous webbing to hierarchical (containing interconnected fine mesh and large channels). Hierarchal pore structure persists in specimens prepared in up to 67% acetone (NGC2), demonstrating that even small quantities of hydrogen bond-donating solvent are sufficient to stabilize these structures. As NGEC is undergoing a clear phase separation from solution to precipitated state, we can assume that such a structure is the result of spinodal decomposition (formation of aggregates possibly induced by crystallization or liquid–liquid phase separation through nucleation and growth of one of the phases).[25,26]

The NGEC highly porous networks of a heterogeneous porous structure are clearly visible in the higher magnification images (right column of Figure 2). The aerogel is composed of long and relatively straight nanofibrils interconnected with each another to form three-dimensional networks with large pore spaces. The pore distribution is very wide, from several nanometers to several micrometers. As it was mentioned in Ref. [24, The mechanism for phase separation-induced gelation of NGEC may be derived from analogous behavior described for cellulose acetate or NC/solvent/nonsolvent.[3,26–29] The robust nature of the NGEC gel structure is probably the result of widespread hydrophobic interactions promoted by the prevalent $-ONO_2$ groups on NGEC chains and hydrogen bonds promoted by hydroxyl groups on ethanol and NGEC chains. As shown in Figure 3, it is assumed that a phase separation between (NGEC+ linked solvents) and (free solvents) has already occurred after partial evaporation of NGEC/acetone/ethanol solution. A porous structure with wide pore size distribution is obtained likely due to the fact that free solvent is first removed and thus making large pores and then the rest of the solvent from NGEC is removed and making small pores.

Powder XRD was also used to determine the effect of the aerogel preparation on the crystalline structure of the NGEC. Figure 4 shows the XRD diagrams of NGEC aerogels, together with those of the starting NGEC powders. Sharp diffraction peaks at 12.98° and diffuse peaks between 15 and 30°, corresponding to (101), and (202), respectively, are observed for all samples. These diffraction peaks indicated that NGEC aerogels clearly retained the crystalline structure of the NGEC. The results of SEM and XRD confirm that the NGEC gels may be formed by aggregation of the NGEC molecules, possibly induced by crystallization as a coherent bulk.[30,31] In addition, the intensity of diffraction peaks at 12.98° decreases as increasing initial ethanol ratio (from NGC1 to NGC4). This may be due to high ethanol content limits the order rearrangement of NGEC molecular, resulting in a relatively decrease in the crystallinity degree of NGEC aerogels. According to papers by Flory, the stiffness of the novel cellulose nitrate chains may be playing a part of role in the formation of crystalline regions at low polymer concentrations.[32,33]

The nitrogen sorption isotherms collected for NGEC aerogels prepared from NGEC/acetone/ethanol solutions with different acetone/ethanol ratios were shown in Figure 5. The isotherms can be classified as Type IV (IUPAC classification) with a Type H1 hysteresis loop, with very large volumes of adsorbed nitrogen at high relative pressures, indicating capillary condensation

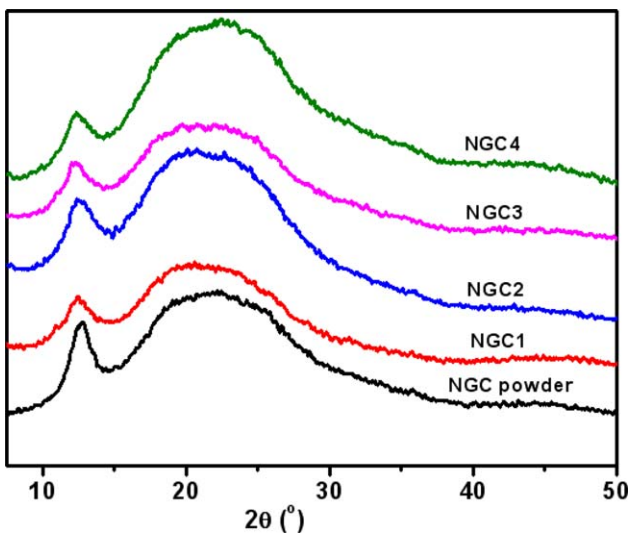

Figure 4. XRD patterns of NGEC powders and NGEC aerogels. [Color figure can be viewed in the online issue, which is available at wileyonlinelibrary.com.]

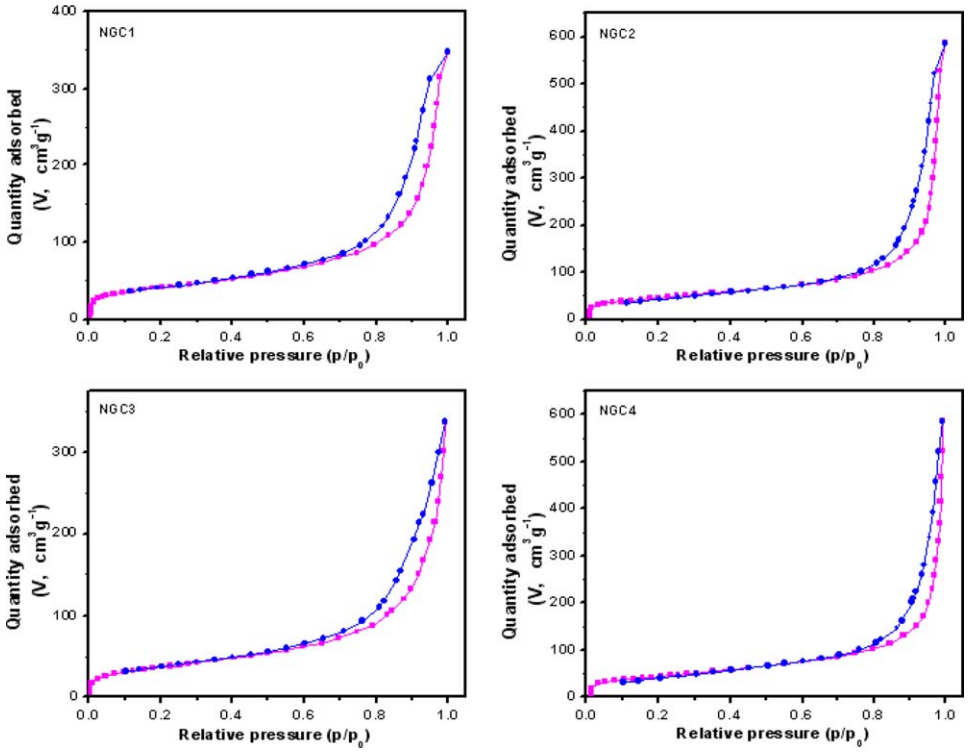

Figure 5. Nitrogen adsorption and desorption isotherms of NGEC aerogels. [Color figure can be viewed in the online issue, which is available at wileyonlinelibrary.com.]

in relatively large pores, as seen in the SEM images. Brunauer–Emmett–Teller (BET) analysis of the amount of N_2 adsorbed at P/P_0 between 0.06 and 0.35 showed that the BET surface area varied between 141 and 183 m^2g^{-1} as shown in Table I, with clear correlation between the initial ethanol ratio and surface area obtained. Initial solvents with reduced ethanol solvent

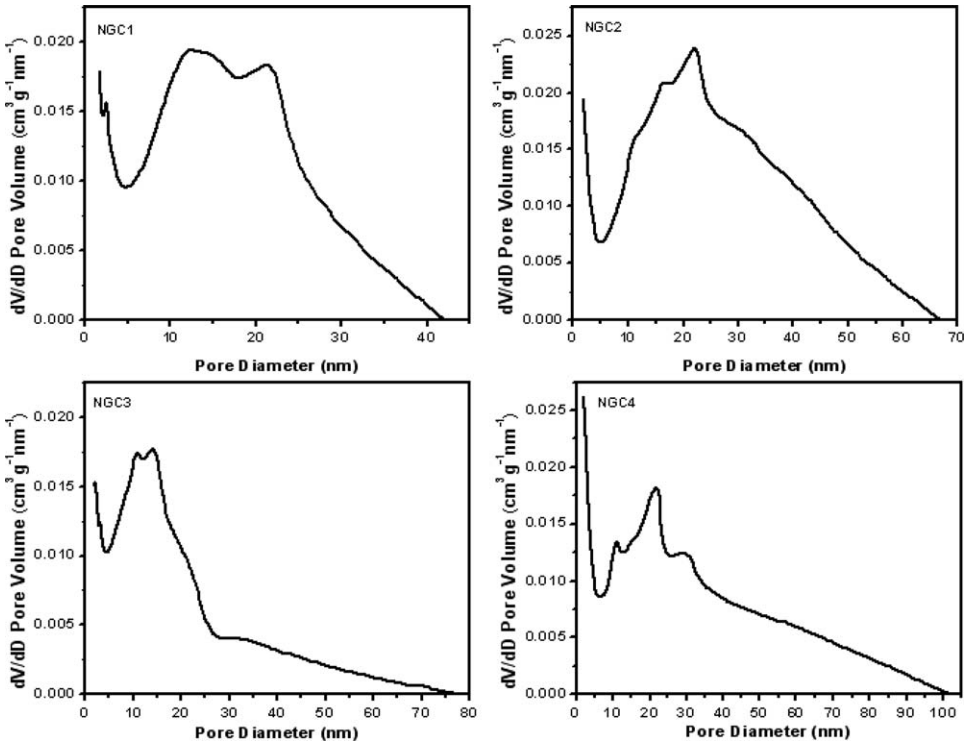

Figure 6. BJH mesopore size distribution for the NGEC aerogels calculated from the desorption branch of the isotherm.

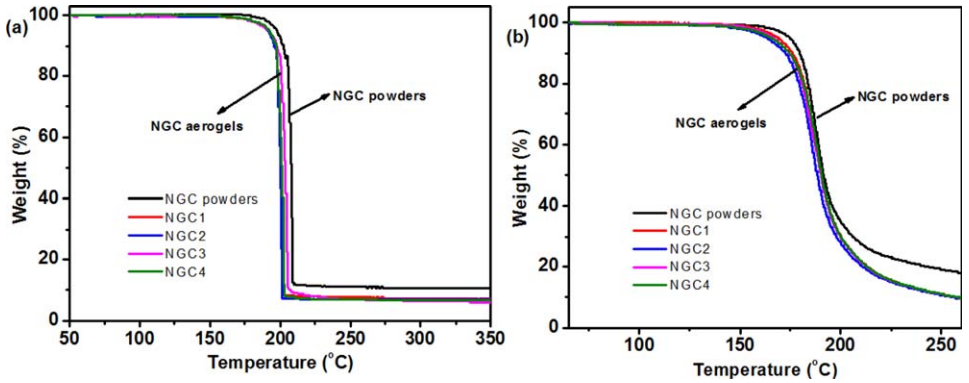

Figure 7. TG/DTA curves for NGEC powders and NGEC aerogels; sample mass 1.0 mg; heating rate a 10°C min^{-1} and b 1°C min^{-1}; nitrogen atmosphere. [Color figure can be viewed in the online issue, which is available at wileyonlinelibrary.com.]

content generated gels with lower surface areas, the lower values is believed to be due to a increase in gel density from 0.082 to 0.179 gcm^{-3} and an increase in the size of the primary network structure with increasing acetone content as shown in SEM images.

Figure 6 further shows the pore size distribution of the aerogels calculated from the desorption branch of the isotherm using BJH analysis.[34] The NGEC aerogels show broad pore size distribution with pores spanning the whole mesopore range, but regular changes are observed for average pore size of NGEC aerogels (Table I). NGEC aerogels with larger average pore diameter, and larger mesopore and macropore volume were obtained from system with higher ethanol content. In detail, with ethanol content increasing, the average pore diameter calculated from BJH analysis increases from 13.8 to 23.0 nm. The total pore volume increases from 0.51 to 0.98 $cm^3\ g^{-1}$ compared to the mesopore volume increases from 0.38 to 0.56 $cm^3\ g^{-1}$ as ethanol content increasing. However, the ratio of mesopore volume to total pore volume decreases from 73.93 to 56.94% though the mesopore volume increases with increasing ethanol content. The differences shown between the total pore volume and mesopore volume of the aerogels (Table I) indicate that there were a significant number of macropores within the samples which is consistent with the SEM image. Taken together, the SEM and physisorption data indicate that shifting initial solvent composition impacts both macropore and mesopore geometries and size distributions in the NGEC aerogels.

Thermogravimetric analysis (TGA) of the aerogel samples (Figure 7) showed that the decomposition profiles of the NGEC powders and aerogels are similar, with a single sharp exothermic behavior accompanied by a sharp weight loss in the TG curve. For the same sample, the maximum mass loss temperature increases with increasing heating rate. Conversely, at the constant heating rate, as shown in Figure 7(a) (10°C min^{-1}), the decomposition temperatures of NGEC aerogel shift to lower temperatures compared to NGEC powders (from 207 to 200°C), which indicate that the thermal decomposition of NGEC aerogel is accelerated and this process becomes more acute. Also, Figure 7(b) shows this result at heating rate of 1°C min^{-1}. This observation may be due to the reason that the high surface area of NGEC aerogels causes an increase in the sample's heat absorption ability and hence lower decomposition temperature.

CONCLUSION

NGEC aerogels are prepared from NGEC alcogels after solvent exchange with ethanol and drying under supercritical CO_2 ($scCO_2$). These aerogels were highly porous, with low densities and moderate surface areas. As indicated by XRD, the NGEC aerogels clearly retained the crystalline structure of the NGEC. The thermal decomposition of NGEC aerogel is accelerated and this process becomes more acute compared to NGEC powders which could prove invaluable in some applications. We also have investigated the influence of initial solvent composition on the properties of NGEC aerogels. This method simultaneously supported NGEC aerogels with moderate surface areas and large mesopore volumes with a combination of large macropore volumes and a wide range of mesopore sizes. NGEC aerogels with large pore size distribution range, average pore diameter, and mesopore and macropore volume were obtained from system with high ethanol content. The capability to easily adjust the pore structures by simple modification of preparative conditions is provided by mixing solvents in different ratios. We intend to investigate potential application of NGEC aerogels as a cheap and convenient moderate surface area material in explosives and propellants, separations, purification science and biomedicine as due to their very simple preparation and tunable pore structures.

REFERENCES

1. Perez-Ramirez, J.; Christensen, C. H.; Egeblad, K.; Christensen, C. H.; Groen, J. C. *Chem. Soc. Rev.* **2008**, *37*, 2530.
2. Shi, Y.; Wan, Y.; Zhao, D. *Chem. Soc. Rev.* **2011**, *40*, 3854.
3. Peterson, G. R.; Cychosz, K. A.; Thommes, M.; Hope-Weeks, L. J. *Chem. Commun.* **2012**, *48*, 11754.
4. Gao, X.; Xu, L. P.; Xue, Z.; Feng, L.; Peng, J.; Wen, Y.; Wang, S.; Zhang, X. *Adv. Mater.* **2014**, *26*, 1771.
5. Hüsing, N.; Schubert, U. *Angew. Chem. Int. Ed.* **1998**, *37*, 22.

6. Bag, S.; Kanatzidis, M. G. *J. Am. Chem. Soc.* **2010**, *132*, 14951.
7. Hardjono, Y.; Sun, H.; Tian, H.; Buckley, C.; Wang, S. *Chem. Eng. J.* **2011**, *174*, 376.
8. Wei, T. Y.; Chen, C. H.; Chien, H. C.; Lu, S. Y.; Hu, C. C. *Adv. Mater.* **2010**, *22*, 347.
9. Kistler, S. *J. Phys. Chem.* **1932**, *36*, 52.
10. Grishechko, L.; Amaral-Labat, G.; Szczurek, A.; Fierro, V.; Kuznetsov, B.; Pizzi, A.; Celzard, A. *Ind. Crops Prod.* **2013**, *41*, 347.
11. Grishechko, L.; Amaral-Labat, G.; Szczurek, A.; Fierro, V.; Kuznetsov, B.; Celzard, A. *Micropor. Mesopor. Mater.* **2013**, *168*, 19.
12. Amaral-Labat, G.; Szczurek, A.; Fierro, V.; Masson, E.; Pizzi, A.; Celzard, A. *Micropor. Mesopor. Mater.* **2012**, *152*, 240.
13. Shao, Z. Q.; Xu, K.; Hao, H. Y.; Wang, J. X. CN1438248. **2007**.
14. Wang, F. J.; Yang, F. F.; Wang, J. N.; Shao, Z. Q. *Chin. J. Explo. Propellant* **2006**, 51.
15. Shao, Z. Q.; Yang, F. F.; Wang, W. J.; Wang, F. J. *Chin. J. Explo. Propellant* **2006**, 55.
16. Shao, Z. Q.; Wang, W. J. Structure and properties of cellulose nitrate. National Defense Industry Press: Beijing, **2011**.
17. Yi, J. H.; Zhao, F. Q.; Xu, S. Y.; Zhang, L. Y.; Gao, H. X.; Hu, R. Z. *J. Hazard. Mater.* **2009**, *165*, 853.
18. Katoh, K.; Ito, S.; Kawaguchi, S.; Higashi, E.; Nakano, K.; Ogata, Y.; Wada, Y. *J. Therm. Anal. Calorim.* **2010**, *100*, 303.
19. Pourmortazavi, S. M.; Hosseini, S. G.; Rahimi-Nasrabadi, M.; Hajimirsadeghi, S. S.; Momenian, H. *J. Hazard. Mater.* **2009**, *162*, 1141.
20. Tappan, B. C.; Brill, T. B. *Propell. Explos. Pyrot.* **2003**, *28*, 223.
21. Li, J.; Brill, T. B. *Propell. Explos. Pyrot.* **2006**, *31*, 61.
22. Jin, M. M.; Luo, Y. J. *Chin. J. Energ. Mater.* **2013**, *21*, 230.
23. Jin, M. M.; Luo, Y. J. *Chin. J. Explos. Propell.* **2013**, *1*, 82.
24. Zhang, Y. H.; Shao, Z. Q.; Gao, K. Z.; Li, J.; Wu, X.; Wang, W. J.; Wang, F.; Liu, Y. *Cellulose* **2014**, *1*, in press.
25. Gavillon, R.; Budtova, T. *Biomacromolecules* **2008**, *9*, 269.
26. Reuvers, A.; Altena, F.; Smolders, C. *J. Polym. Sci. Part B: Polym. Phys.* **1986**, *24*, 793.
27. Hao, J. H.; Wang, S. *J. Appl. Polym. Sci.* **2001**, *80*, 1650.
28. Appaw, C.; Gilbert, R. D.; Khan, S. A. *Biomacromolecules* **2007**, *8*, 1541.
29. Appaw, C.; Gilbert, R. D.; Khan, S. A.; Kadla, J. F. *Cellulose* **2010**, *17*, 533.
30. Heath, L.; Zhu, L.; Thielemans, W. *Chem. Sus. Chem.* **2013**, *6*, 537.
31. Heath, L.; Thielemans, W. *Green Chem.* **2010**, *12*, 1448.
32. Flory, P. J. *Trans. Faraday Soc.* **1955**, *51*, 848.
33. Shultz, A.; Flory, P. *J. Polym. Sci.* **1955**, *15*, 231.
34. Barrett, E. P.; Joyner, L. G.; Halenda, P. P. *J. Am. Chem. Soc.* **1951**, *73*, 373.